Joint energy demand and thermal comfort optimization in photovoltaic-equipped interconnected microgrids

Baldi, S; Karagevrekis, A; Michailidis, IT; Kosmatopoulos, EB

DOI
10.1016/j.enconman.2015.05.049

Publication date
2015

Document Version
Accepted author manuscript

Published in
Energy Conversion and Management

Link to formal publication Reliability Engineering & System Safety (Elsevier): http://dx.doi.org/10.1016/j.enconman.2015.05.049

Joint Energy Demand and Thermal Comfort Optimization in Photovoltaic-equipped Interconnected Microgrids

Simone Baldi[a,c][1], Athanasios Karagevrekis[b], Iakovos T. Michailidis[a,b] and Elias B. Kosmatopoulos[a,b]

[a] Information Technologies Institute (I.T.I.), Centre of Research & Technology – Hellas (CE.R.T.H.), Thessaloniki, Greece
[b] Department of Electrical and Computer Engineering, Democritus University of Thrace, Xanthi, Greece
[c] Delft Center for Systems and Control, Delft University of Technology, The Netherlands

***Abstract*— Electrical smart microgrids equipped with small-scale renewable-energy generation systems are emerging progressively as an alternative or an enhancement to the central electrical grid: due to the intermittent nature of the renewable energy sources, appropriate algorithms are required to integrate these two typologies of grids and, in particular, to perform efficiently dynamic energy demand and distributed generation management, while guaranteeing satisfactory thermal comfort for the occupants. This paper presents a novel control algorithm for joint energy demand and thermal comfort optimization in photovoltaic-equipped interconnected microgrids. Energy demand shaping is achieved via an intelligent control mechanism for heating, ventilating, and air conditioning units. The intelligent control mechanism takes into account the available solar energy, the building dynamics and the thermal comfort of the buildings' occupants. The control design is accomplished in a simulation-based fashion using an energy simulation model, developed in EnergyPlus, of an interconnected microgrid. Rather than focusing only on how each building behaves individually, the optimization algorithm employs a central controller that allows interaction among the buildings of the microgrid. The control objective is to optimize the aggregate microgrid performance. Simulation results demonstrate that the optimization algorithm efficiently integrates the microgrid with the photovoltaic system that provides free electric energy: in particular, for each building composing the microgrid, the energy absorbed from the main grid is minimized, the energy demand is balanced with the solar energy delivered to each building, while taking into account the thermal comfort of the occupants.**

***Index Terms*— Interconnected microgrids, demand response, thermal comfort.**

I. Introduction

Increasing energy demand and more strict environmental regulations are enabling the transition from traditional electrical grids with centralized power plants to smart electrical microdgrids where the existing power grid is enhanced with distributed, small-scale renewable-energy generation systems [1]. This so-called smart grid paradigm is emerging progressively: currently, many microgrids are connected to the existing grid, allowing the two grids to coexist until eventually the load will migrate to the new grid [2]. In this hybrid intermediate state, the energy produced from the microgrid renewables can be used to reduce dependence on grid-supplied energy. On the other hand, the use of renewables inserts uncertainty into the system, due to their stochastic output profile. In some cases electric utilities raise reservations on distributed energy generation since

[1] Corresponding author: s.baldi@tudelft.nl

the lack of monitoring and control of these energy sources might contribute to the instability of the electric grid [3]. For these reasons, one of the main challenges in the development of microgrids is to deploy control systems that take the appropriate decisions for energy distribution and consumption: these tasks are also referred to as distributed generation (DG) and demand response (DR) tasks, and a strategy addressing these tasks can be referred to as DG/DR management strategy or DG/DR control strategy.

The management of distributed generation and demand response in microgrids implies interactions between the demand and the supply side. The power provider must dynamically change the load for their users, otherwise energy might be wasted by some users (because of redundant power), while lack of power will occur for other users [4]. A typical way through which the demand side interacts with supply side is via intelligent load managing and scheduling [5]. Several approaches to optimal scheduling of microgrid energy consumption have been proposed: the evaluation of the effectiveness of DG/DR solutions is based on performance metrics like service quality, electricity consumption and price [6]. Without aiming at being exhaustive, only approaches that rely on simulation-based optimization procedures to maximize the microgrid performance are addressed in this work: with simulation-based optimization it is meant an approach that exploits the availability of a model of the microgrid to perform simulations and to assess the performance of a particular DG/DR management strategy. Two main families can be identified: DG/DR management based on receding horizon optimization and DG/DR management based on co-simulation.

In DG/DR management based on receding horizon optimization a model of the microgrid is used at every time step in a receding horizon fashion to evaluate and optimize the performance of the management strategy: in [7] minimization the cost of electricity and natural gas for building operation while satisfying the energy balance and operating constraints of energy supply equipment and devices is considered. The uncertainties are captured and their impact is analyzed by the scenario tree method. In [8] a mixed integer linear programming (MILP) approach is used to schedule distributed energy resources operation and electricity-consumption household tasks so as to minimize a one-day forecasted energy consumption cost. In [9] the model predictive control (MPC) approach is applied for achieving economic efficiency in a microgrid with storages and controllable loads. In [10] an energy management algorithm based on mixed-integer nonlinear programming (MINLP) schedules the microgrid generation in a local energy market so as to maximize the utilization of distributed energy resources. In DG/DR management based on co-simulation elaborate microgrid models, developed using EnergyPlus [11], TRNSYS [12], and other programs [13], are coupled together with gradient-free optimization methods, using software environments like BCVTB [14]. Gradient-free optimization methods (e.g. genetic algorithms, Nelder-

Mead method, particle swarm optimization, pattern search) are used to evaluate and optimize the performance of the management strategy. In [15] a simulation based control scheme is used to improve management rules for a low-energy building controlled by a hierarchical fuzzy rule-based controller. The authors of [16] adopt co-simulation to reduce energy consumption and occupant discomfort via management of heating, ventilating, and air conditioning (HVAC) systems. The controller of [17] utilizes an optimizer to minimize an electric cost-based objective function whose evaluation involves simulation of the building energy system. In [18] power imbalance between supply and demand sides is regulated via an interactive building power demand management strategy for the interaction of commercial buildings with a smart grid. In [19] a modified simulated annealing triple-optimizer is introduced to find the optimal energy management strategy in terms of financial gain maximization in photovoltaics-supplied microgrids in a variable grid price scenario.

Both receding horizon-based and co-simulation-based approaches rely on some model to predict the effect of a control policy in the future: in general, the energy-efficient control is performed in an open-loop fashion in the receding horizon case, and in a closed-loop feedback fashion using parameterized policies in the co-simulation case. In both approaches the curse of dimensionality emerges as the main problem. In fact, receding-horizon control needs simplified (often linearized) models so as to address the real-time requirements of the control problem: the adoption of more realistic nonlinear models makes the computations impossible to be solved in real-time. In the co-simulation case the problems are associated to the large number of policy parameters to be optimized and to the fact that gradient-free optimization methods do not scale to large-scale instances.

Furthermore, while the vast majority of literature addresses minimizing of microgrid running costs, power consumption and reduction of the peak demand from the central grid, only a subset of DG/DR management strategy performs the DG/DR tasks while taking into account the end-user (building occupant) thermal comfort. It is recognized that end-user thermal comfort is a critical factor in determining the energy consumption in a microgrid. Local sensation [20] and comfort [21] of individual body parts, as well as whole-body sensation and comfort [22], influence the behavior of occupants: a large proportion of energy must be used for building climate control purposes to keep occupants thermally satisfied [23]. According to the EN15251 standard [24] and to the Renewable Energy Road Map [25] thermal comfort should not be violated except for small intervals during the building operation. In that sense, thermal comfort constraints should be satisfied by all acceptable DG/DR control strategies. The DG/DR management approaches that try to take thermal comfort into account often rely on dry-bulb temperature tracking as a comfort-maintaining criterion: a few examples include the model-based predictive controllers of [26], the stochastic model predictive controller of [27], the parallel model-

based predictive controller based on Lagrangian dual method of [28], or the multi-objective genetic algorithm of [29]. By relying only on dry-bulb temperature tracking, they neglect humidity and radiant temperatures that can lead in practice to insufficient estimation of actual thermal comfort. An exception is represented by the model predictive controller of [30], where the occupants' thermal comfort sensation is addressed by the comfort index known as predicted mean vote (PMV): however, here the management problem is limited to one thermal zone with one actuator. More realistic estimate of thermal comfort can be achieved via: the predicted mean vote, also known as Fanger index, adopted both in the ASHRAE 55-2004 standard [31] and in the ENISO 7730 standard; the two-node model of human thermoregulation [33]; or the adaptive thermal comfort model added in the ASHRAE-55 2010 standard and based on mean outdoor temperature [34].

This work proposes a novel algorithm for optimal management of heating, ventilation, and air conditioning units in photovoltaic-equipped interconnected microgrids. Demand response management is achieved since, via regulation of the HVAC set point, the energy demand of the HVAC units and thus of the buildings is regulated (HVAC operation account for 50% of the energy demand of a building [35]). Distributed generation management or solar energy is achieved since every building, equipped with its own photovoltaic panel, is allowed to exchange energy with the other buildings. Demand response and distributed generation are optimized while guaranteeing acceptable thermal comfort conditions for the end users in terms of the Fanger index. A test case consisting of a microgrid with three buildings connected both to photovoltaic arrays and to the central electrical grid is used to evaluate the effectiveness of the proposed algorithm. The microgrid test case has been developed in EnergyPlus and it assumes the presence of a central controller that allows exchange of information and interaction among the buildings of the microgrid (fully-interconnected microgrid): rather than focusing on how each building behaves individually, the objective of demand response and distributed generation control strategy is to optimize the aggregate microgrid performance. The buildings should try to satisfy their needs using only the solar energy from the photovoltaic panels: a building that does not receive enough solar energy will have to buy extra energy from the central grid. The final objective is not only to manage the HVAC set points so as to reduce the energy absorbed from the central electrical grid, but also to guarantee acceptable thermal comfort conditions. The work has both a theoretical and an applied intent. From the theoretical side, the proposed system uses a simulation-based optimization procedure which aims at solving adaptively the Hamilton-Jacobi-Bellman (HJB) equation associated with the optimal control problem: the DG/DR tasks are parameterized in terms of the value function, and the proposed algorithm, namely Parameterized Cognitive Adaptive Optimization (PCAO) updates the value function in such a way to approach the solution of the HJB

equation, thus achieving the optimal DG/DR control strategy. From the applied side, the energy demand and thermal comfort optimization is performed jointly: the proposed algorithm is shown to be able to handle the nonlinear and mutually interconnected nature of the tasks, and to be able to exploit the interconnections so as to optimize the microgrid aggregate performance. In order to explain the complex and interconnected nature of the problem it is shown that any optimization of the demand response side that does not take into account the distributed generation side (i.e. buildings optimize the HVAC set points without exchanging solar energy among each other) and any optimization of the distributed generation side that does not take into account the demand response side (i.e. buildings exchange solar energy under simple HVAC rule-based control) leads to far from optimal solutions. The simulation-based optimization used in this application is based on an adaptive optimization algorithm that has been developed and tested by the authors in different real-life large scale applications: traffic light management [36], control of robotic swarm [37], HVAC regulation in single thermal zones [38], conventional [39] and high-inertia office buildings [40]. The paper is organized as follows: Section II describes the problem setting and the control objectives. In Section III the optimization algorithm is presented. Section IV shows the simulation results. Section V concludes the paper.

II. Problem Description

The microgrid used for the evaluation of the proposed control algorithm is composed of three commercial buildings which are connected both to photovoltaic panels and to the central electrical grid. The microgrid uses the electricity of the photovoltaic panels to fulfil its needs: if such power is not enough, the microgrid must absorb the necessary power from the central electrical grid. As shown in table I, each building of the microgrid is composed of ten thermal zones; each building is equipped with an HVAC unit whose operation can be regulated via ten temperature set points (one for each thermal zone). Each building has different energy needs. This is mainly due to the fact the buildings have different sizes. In particular, as can be seen in table I, the buildings cover a surface of 200 m^2, 365 m^2, and 100 m^2, respectively. Because of the different sizes, each building mounts a different HVAC system, absorbing a maximum of 8.000, 15.000 and 4.000 BTU per hour, respectively. The second building, being the largest one, is equipped with a more powerful HVAC system that is able to satisfy the thermal needs of larger thermal zones. The HVAC system of the third building, on the other side, is less powerful than the other HVAC systems.

It is assumed that the HVAC units are the only controllable loads of the buildings: the HVAC units can be controlled via the temperature set point. During occupancy hours, an uncontrollable base load also is present. Since the buildings host commercial activities, the occupancy schedule is 7.30am-4pm, and the base load is a

constant load of 2 kW, 4 kW and 1 kW respectively, from 6am to 6pm. The uncontrollable base load is constant as typically happening in commercial activities [41]. The base load acts for some time outside the occupancy schedule in order to take into account extended operational time of appliances and machines. For similar reasons the HVACs are operated from 6am to 6pm, in order to accommodate for precooling actions and for possibly early/late workers. All the elements of the microgrid have been modelled and simulated using EnergyPlus; the microgrid is supposed to be located in Athens, Greece. Historical weather data collected during summer 2011 and retrieved form the EnergyPlus website [42] are used in the simulations.

Table I. Microgrid test case (commercial buildings, occupancy schedule 7.30am-4pm)

	Size	**No. Thermal zones**	**No. HVAC set points**	**Power HVAC units**	**Size solar panel**	**Base load (uncontrollable) 6am-6pm**
Building #1	200 m^2	10	10	8.000 BTU per hour	30 m^2	2 kW
Building #2	365 m^2	10	10	15.000 BTU per hour	55 m^2	4 kW
Building #3	100 m^2	10	10	4.000 BTU per hour	15 m^2	1 kW

The fact that each building has a different energy demand has been assembled intentionally so as to make the DG/DR control problem more challenging. As a matter of fact, the distribution of the solar energy among the three buildings plays a very important role. It is assumed that each building is equipped with its own solar panel, of 30 m^2, 55 m^2, and 15 m^2, respectively. The proportion 30%-55%-15% has been chosen to match the proportion of the size of the buildings (200 m^2, 365 m^2, and 100 m^2, respectively). In this work, two settings will be considered with respect to the solar energy distribution. In the first setting, each building will use exclusively the energy from its own panel without sharing any portion of energy with the other buildings. This setting is referred to as the *isolated setting*. In the second setting, the buildings can share their energy with the other buildings (according to the Kirchhoff's circuit laws). Since the buildings are assumed to be close to each other, no transportation losses in exchanging solar energy are considered. This second setting is referred to as the *connected setting*. When the solar power delivered to a building exceeds the building demand, it is assumed that the excess of power is dissipated as heat in the devices of the buildings (wasted redundant power) or that some safety device will be activated to dissipate it. No excess of electric power from the main grid is considered, since it is assumed that such excess is managed and regulated by the power utility. Intuitively, the isolated and connected settings will lead to very different results. In particular, the isolated setting is expected to waste more power. The connected setting allows for more flexibility since, depending on the requirements of each building, the photovoltaic energy can be distributed to the buildings in the right amount needed. The isolated setting represents an individual microgrid where each customer communicates with the energy source individually and

individually controls its energy demand. In the connected setting it is assumed that the grid is fully-interconnected, so that there is a central control unit that knows the thermal state of all buildings, as well as the external weather conditions and the available solar energy: via interactions among users and information exchange, a demand response/distributed generation program has the objective to optimize the aggregate microgrid performance. In the following, the demand response/distributed generation program of the microgrid is defined and the control actions that can be taken by the program in order to optimize the aggregate microgrid performance are explained.

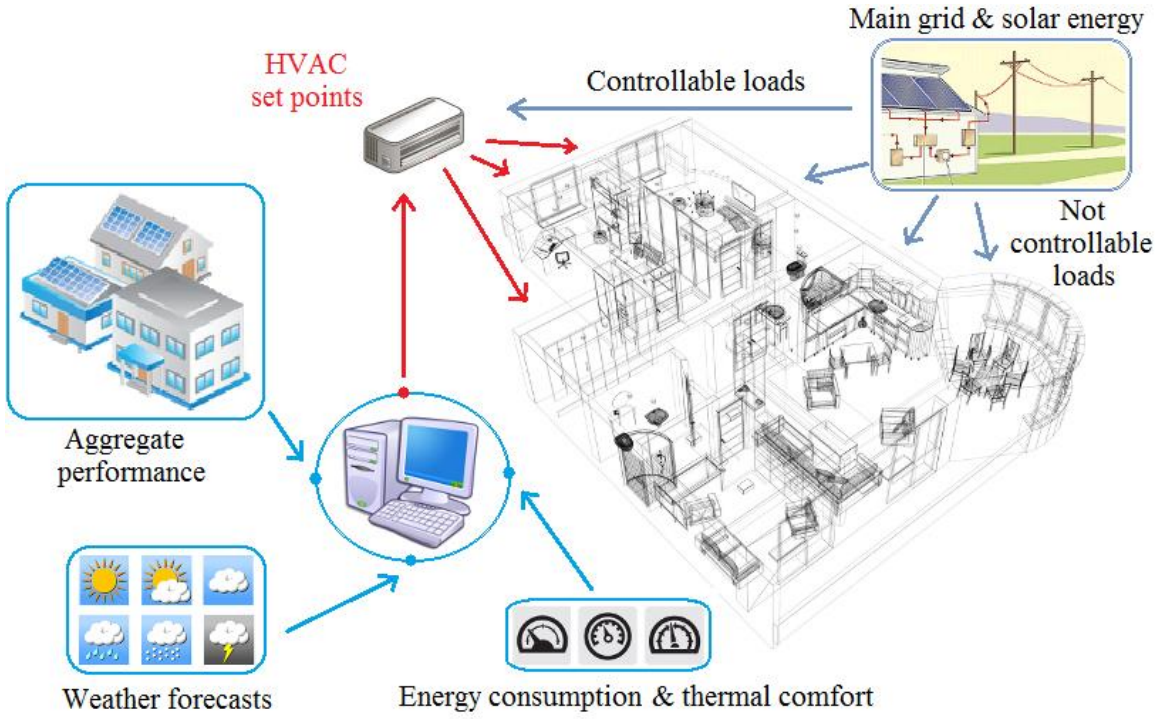

Figure 1. Demand response and distributed generation in a building of the microgrid

1. Manipulable Inputs

As the microgrid is tested during summer, the HVAC is used purely for cooling purposes. In the proposed microgrid, the task of a controller is to regulate thirty manipulable control inputs, i.e. the HVAC temperature set points in each thermal zone of the microgrid, for a total of thirty set points (figure 1). Via the regulation of the temperature set points, the controller is responsible (directly and indirectly) for two tasks:

1. Demand response task (DR): the controller influences directly the energy demand of the HVAC systems, and thus a big portion of the energy demand of the buildings (in real life HVAC operation account for 50% of the total energy used in a building);

2. Distributed generation task (DG): the controller influences indirectly the way energy will be absorbed from the main grid and from the photovoltaic panels (either in the isolated or in the connected setting) or the way energy will be shared among buildings (in the connected setting).

It must be underlined that the DG and DR tasks are strongly interconnected and influence each other. In the connected setting, a building with a big energy demand will require a large amount of solar energy from the photovoltaic arrays, and might prevent the microgrid from satisfying the aggregate energy need using only solar energy: as a consequence, the microgrid will need to absorb energy from the central electrical grid. Through an optimal DG and DR management, the controller must achieve the following goals:

a. *Energy consumption:* dynamically shape the energy demand of each building;
b. *Energy distribution:* dynamically exploit the photovoltaic energy among the buildings;
c. *Energy cost:* match the demand with the supply of solar energy so as to minimize the energy absorbed from the central grid;
d. *User thermal comfort:* guarantee thermal satisfaction of the buildings' occupants.

These tasks are quantified in the next section introducing the aggregate performance index of the microgrid.

2. Performance Index

The solution to the optimization problem of consumption - distribution - cost - comfort can be translated to finding the global minimum of a given *objective function*. The function expresses the performance of building *#i* and of the aggregate microgrid, and consists of a power cost term and of a thermal comfort term:

$$Tot_i(t) = E_i(t) + C_i(t), \qquad Tot(t) = \sum_{i=1}^{3} E_i(t) + C_i(t) \tag{1}$$

At time *t*, E_i is given in kW and C_i in percentage of dissatisfied persons. As the daily power consumption of the microgrid is of the order of tens of kW, and the thermal comfort is a percentage typically lying between 0 and 15%, the two terms are of a similar order of magnitude and no additional scaling is adopted. In principle, a scaling factor between the two terms in (1) can be introduced in order to emphasize a term with respect to the other. The cost in (1) is then summed up for every building, and then integrated over the entire day. The integral of the power cost term over time will give the energy consumption: for this reason, the notation E_i is used in (1), where E stands for energy. In the following, the terms energy demand and power demand will be used almost interchangeably. It must be noticed that, generally speaking, the two terms in (1) play an antagonistic role: in order to keep the user satisfied (from a thermal comfort point of view) large amounts of energy are typically

required. Vice versa, management strategies giving emphasis to the reduction of the energy consumption typically need to sacrifice the thermal comfort of the users. However, these are just general considerations, since the total cost in (1) is not a static function, but it is subjected to the thermal dynamics of the buildings. Two management strategies that require very similar amounts of energy might achieve totally different comfort scores, according to how the energy is distributed throughout the day and among the buildings.

1) Power Cost E_i

The power cost of each building depends on the power demand d_i of the building (e.g. the power requested by the HVAC unit and by the uncontrollable load) and on the solar power s_i delivered to the building. Formally:

$$E_i = max\,(0,\ d_i - s_i) \tag{2}$$

Equation (2) shows that, when the power consumption of a certain building is higher than the solar power that is delivered to it, the power cost is the difference between these two quantities. This difference can be called *effective power*, since it represents the power which is effectively paid in the bill. Otherwise, if the power consumption of the building is smaller than the solar power that is delivered, the cost is 0, because the building can completely satisfies its needs using only the solar power. The solar power is assumed to be free of charge (no charge in the bill), while only the power absorbed from the central electrical grid is paid (when $d_i > s_i$). Note that s_i is determined according to the particular adopted DG strategy: for example, a building can use exclusively the power generated by its own photovoltaic panel (in the isolated setting) or absorb a portion of the total solar power of the microgrid according to the Kirchhoff's circuit laws (in the connected setting). It is important to notice that, in the isolated setting, the sum of (2) over every building in the microgrid is different than the difference between the total power demand of the microgrid and the total solar power. In fact, (2) considers the possibility that power might be in excess in some buildings (when $d_i < s_i$), while lack of power might occur in other ones (when $d_i > s_i$). When $d_i < s_i$, the excess of power is *redundant power* or wasted redundant power. In fact, it is assumed that the redundant power in one building is completely wasted (via heat in appliances or via safety devices that dissipate excess of power). To reduce the amount of wasted redundant power and improve grid stability, we impose the constraint:

$$(s_i - d_i)/d_i < 15\% \tag{3}$$

at each timestep. Adopting the model described in [43], the photovoltaic generation is modelled according to the following equation:

$$s_i = \eta\, S_i\, \alpha\, I_\alpha\ (1 - 0.005\ (t_0 - 25)) \quad (4)$$

where, η is the conversion efficiency of photovoltaic array (%), S_i is the array area (in m^2) of the array #*i*, I_α is the solar radiation (in kW/m^2), t_0 is the outside air temperature (in °C). No transportation losses between buildings are assumed. Conversion losses are modelled via the conversion efficiency η. It is also assumed that the photovoltaic panels are oriented in the same direction and receive the same amount of solar radiation (different orientations can be taken into account by modifying the solar radiation I_α with the position of the sun). The power demand of the microgrid is the sum of the HVACs power demand and the uncontrollable loads: several studies reveal that in most commercial application HVAC units are the only controllable loads, and that HVAC operation accounts for 50% the total building energy demand, with peaks of 70% during summer [35]. It is finally emphasized that the microgrid test case does not consider the presence of distributed electric storage devices. This is an intentional choice led by both practical and theoretical reasons. From the practical side, state-of-the-art electric storage devices have a short life [44] and technological research on storage devices is still going on [45]. From the theoretical side, it is interesting to study to what extent an optimal DG/DR control strategy can shape the demand of the microgrid and reduce dependence on the central grid-supplied energy without the aid of storage devices. Summarizing, minimization of (2) takes into account the goals of energy consumption (a) and energy cost (c) directly, and the goal of energy distribution (b) indirectly.

2) Thermal Comfort Cost C_i

Povl Ole Fanger (1934-2006) elaborated in the 70's a model for general thermal satisfaction called Predictive Mean Vote (PVM). The PMV is the index that provides the average thermal sensation through voting by a large group of people, expressed in the 7-point ASHRAE scale (+3 till -3, where +3=hot and -3=cold), for each combination of thermal environmental variables, their activity and clothing. The PMV model is based on the Fanger's comfort equation, derived by combining six parameters (air temperature, mean radiant temperature, relative humidity, air speed, metabolic rate, and clothing insulation). According to EN15251 standard [24] and to the Renewable Energy Road Map [25], in order to ensure a comfortable indoor environment, the PMV must be maintained at 0 in the 7-point ASHRAE scale, with a tolerance of ± 0.5 units. These limits should not be violated except for small intervals during the building operation. Instead of the PMV scale, it is more convenient to calculate the number of persons that are dissatisfied with a certain indoor environment: to this purpose the Predicted Percentage of Dissatisfied people (PPD) is defined via:

$$C_i = PPD = 100 - 95 \times e^{(-0.03353 \times PMV^4) - 0.2179 \times PMV^2)} \quad (5)$$

To achieve acceptable thermal conditions (± 0.5 units of PMV), the PPD must be kept approximately below 10%, as shown in figure 2. Only temporary violations are admitted, while the average PPD should be kept below the 10% threshold. In order to limit temporary violation of PPD we impose the constraint:

$$C_i < 15\% \quad (6)$$

at each timestep. This is suggested because otherwise dissatisfied people would overrule the decision of the DG/DR controller and alter the operation of the HVAC (e.g. by opening windows or by manually changing set points). Summarizing, minimization of (5) takes directly into account the goal of thermal comfort (d).

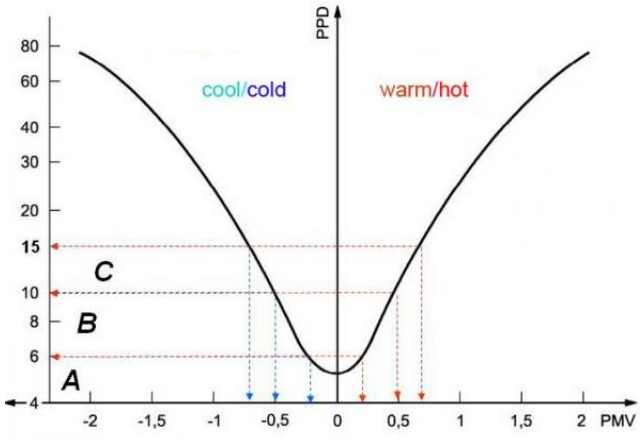

Figure 2. Relationship between PMV and PPD

3. Base Case Scenarios

For comparison purposes, apart from the proposed method, four other DG/DR strategies have been tested. These four scenarios are summarized as follows:

- *Scenario 24-isolated*: For every thermal zone, set the temperature set points of each HVAC unit at 24^{o} C (during the period from 6 am to 6 pm). Besides, deliver 30% of the total solar energy to the first building, 55% to the second building, and the remaining 15% to the third;
- *Scenario 25-isolated*: For every thermal zone, set the temperature set points of each HVAC unit at 25^{o} C (during the period from 6 am to 6 pm). Besides, deliver 30% of the total solar energy to the first building, 55% to the second building, and the remaining 15% to the third.
- *Scenario 24-connected*: For every thermal zone, set the temperature set point of each HVAC unit at 24^{o} C (during the period from 6 am to 6 pm). Besides, distribute the total solar energy proportionally to the energy demand of each building;

- *Scenario 25-connected*: For every thermal zone, set the temperature set point of each HVAC unit at 25^{o} C (during the period from 6 am to 6 pm). Besides, distribute the total solar energy proportionally to the energy demand of each building.

The terms "isolated" and "connected" indicate two different distributed generation strategies, while "24^{o} C" and "25^{o} C" indicate two different demand response strategies. The combination of these strategies gives rise to four different DG/DR control scenarios. With respect to the distributed generation strategies, it can be seen that the first two scenarios (24-isolated and 25-isolated) distribute the solar energy according to the proportion of the size of the solar panels, which mimes the proportion of the size of each building. That is, it is assumed that buildings use solar energy from their own panel without sharing solar energy among each other. This is a popular solution in most microgrids. However, it will be demonstrated that these two scenarios lead far from optimal results, since the optimal distribution cannot be constant but it must change during the day according to the energy demand of each building. The last two scenarios (24-connected and 25-connected) assume that the total solar energy will be distributed proportionally to the energy demand of each building, according to the Kirchhoff's circuit laws. That is, each building can share the energy generated by its own panel with the other buildings of the microgrid. The solar energy coming from this unique pool will be drawn by each building proportionally to their energy demand, according to the Kirchhoff's circuit laws. It will be demonstrated that, despite the improved performance of these two scenarios, results are far from optimal if the demand response of each building is not appropriately managed.

With respect to the HVAC set points, it can be seen that the four control strategies suggest easy and common usage of HVACs, consisting of keeping the set point constant during office hours. These simple strategies are actually adopted in many real buildings. Some scenarios are more oriented toward thermal comfort at the expenses of energy consumption (24^{o} C); some other scenarios sacrifice thermal comfort so as to have reduced energy consumption (25^{o} C). It has to be noticed that in the four scenarios only the set points 24^{o} C and 25^{o} C have been chosen, because they lead to an acceptable trade-off energy/comfort: in fact, a constant set point at 23^{o} C leads to high energy consumption, while the constant set point 26^{o} C leads to unacceptable thermal conditions. The objective of this work is to find the optimal DG/DR strategy that minimizes (1). It will be demonstrated that the optimal DG/DR strategy is none of the four base case scenarios. The reason for this is that, in order to minimize (1), an intelligent DG/DR strategy must be developed that dynamically distributes the solar energy proportionally to the energy demand of each building, and at the same time dynamically changes the HVAC set points taking into account the building dynamics and the available solar energy. The control

algorithm aiming at minimizing (1) is proposed in the following section.

III. THE PCAO ALGORITHM

Most of conventional control techniques that operate in real buildings achieve far from optimal performance: one of the main reason is that they employ decentralized control strategies for a single thermal zone, and they do not exchange information about what is happening in the other zones. This is also the case of the four scenarios that have been presented, which keep the HVAC set point in a thermal zone constant, no matter what is happening in the other thermal zones. Another important problem leading to far from optimal performance is that model-based control approaches typically employ very simple building models, mostly linear or based on the thermal resistance-capacitance (RC) paradigm. Such models are not always able to catch the complex building dynamics, thus leading to sub-optimal solutions. In order to address and possibly overcome such drawbacks, the objective is to develop a novel DG/DR control strategy under the following settings:

- The control strategy is centralized, thus it operates according to a global state vector containing the thermal state of the entire microgrid (temperature and humidity of the thermal zones), as well as external weather conditions.
- The control strategy is optimized via a simulation-based iterative procedure composed of: evaluating the current control strategy via an elaborate building simulation environment (EnergyPlus in our case), and; updating of the control strategy in such a way to improve performance at the next iteration.

Both these settings requires more complex and difficult programming methods than decentralized methods: however, they give the possibility to catch and exploit in an optimal way the energy transfer between the thermal zones, thus achieving better performance. Similarly to all simulation-based procedures, the model is exploited to run simulations and to predict the future performance of a given control strategy. The control strategy proposed in this work, namely Parameterized Cognitive Adaptive Optimization (PCAO), enjoys the following features: (1) the solution to the Hamilton-Jacobi-Bellman (HJB) equation [46] associated with the optimal control problem is found iteratively; (2) the DG/DR tasks are parameterized in terms of the value function, and the proposed algorithm uses simulations to update the value function in such a way to approach the solution of the HJB equation.

PCAO is a data-driven optimization procedure that can handle models built in elaborate simulations environments; the optimization is performed by accessing the thermal states of the microgrid in a “plug-n-play” fashion. Furthermore, PCAO has demonstrated to be able to handle large-scale optimization problems, which

cannot be handled efficiently using other global optimizers: comparisons with the Nelder-Mead method are shown in [47], while comparisons with the genetic algorithm are carried out in [48]. In the following sections the problem formulation, algorithm and dimension of the problem at hand are presented in details.

1. Problem formulation

The analysis of the optimization algorithm is carried out supposing that the state can be measured. Based on these assumptions, the building dynamics are taken in the following form

$$\frac{d}{dt}x\,(t) = F(x(t), u(t)) \qquad (7)$$

$$H(x, u) \leq 0$$

where *x, u* are the state and the control vectors, respectively; *F, H* correspond to the dynamics and constraints of the system, respectively (implemented via the EnergyPlus simulator). The state comprises external weather conditions, weather forecasts, zone temperature and humidity: the control input comprises the HVAC set-points. The following constraints have been considered:

- Constraint (6): instantaneous PPD value in each building < 15%;
- Constraint (3): instantaneous excess of power $(s_i - d_i)/d_i$ in each building < 15%;

The constraints act at the level of each building. The first constraint has been considered since, even if temporary violations of the 10% threshold are considered, it is preferred such violations not being greater than 15% (cf. figure 2). The second constraint has been considered since most equipment is designed to operate within ± 5-10% of nominal power; the "extra power" usually gets dissipated as heat in the device itself. Assuming that some extra dissipation mechanisms are implemented in the grid, excess of energy less than 15% is considered in order to avoid going beyond the tolerance of the devices, which might overheat or burn. The dynamics and constraints of the system are implemented via the EnergyPlus simulator. The system performance in a simulation period can be described as follows:

$$\mathrm{J} = \int_0^\infty \Pi(\mathrm{x(s)}, \mathrm{u(s)})\mathrm{ds} \qquad (8)$$

where Π is the analytical form of the cost function in (1). After simple mathematic manipulations similarly to [49] (i.e. the introduction of a fictitious filtered version of the input u), the system is transformed into:

$$\frac{d}{dt}x(t) = f(x(t)) + Bu(t) \tag{9}$$

where *x, u* are transformed state vector and control, and *f* contains the transformed nonlinear dynamics (which are assumed to be unknown). The vector $B = [0\ I]^T$ is known. The performance index becomes

$$\mathrm{J} = \int_0^\infty \Pi(\mathrm{x(s)})\mathrm{ds} \tag{10}$$

where the constraints $C(x,u)$ in (7) are included in (10) as penalty functions. The following analysis is carried out based on (9) and (10).

2. Control equations

Although the approach that is presented can be implemented in a variety of nonlinear controllers (PieceWise Linear Control, PieceWise Nonlinear Control, etc.), for simplicity it is presented for the case where a linear controller can achieve satisfactory performance. The interested reader is referred to [50,52] for more general formulations. In fact, a linear controller has been verified to bring relevant improvements in the microgrid. The basic form of the linear controller to be optimized is as follows:

$$u = -B^T P\, x \tag{11}$$

where *x, u* are the states (external weather conditions, indoor temperature and humidity) and control inputs (HVAC set points, percentage of delivered solar energy) of the system; *P* is a positive definite matrix to be optimized. In fact, following a dynamics programming approach [46], according to HJB equation, the controller optimizes the performance of the system is the solution of the following differential equation (The * indicates the optimal value):

$$V^*(x(t)) = \left(\frac{dV^*}{dx}\right)^T (f(x) + Bu^*) = -\Pi(x) \tag{12}$$

where $V^* = x^T P^* x$ is the optimal cost function and $u^* = -B^T P^*\, x$ is the optimal control. The optimal control matrix P^* is found adaptively, by employing the algorithm described in table II and figure 3, and briefly introduced in the next section.

Table II. The PCAO algorithm

Initialize	a) Set *t =0.* b) select two positive constants $e_1 \le e_2$ and a positive number T_h

	c) The matrix $\widehat{P}(0)$ is initialized with a positive definite matrix satisfying: $e_1 I \leq \widehat{P}(0) \leq e_2 I$ d) Set a positive function $a(t)$, which is a constant positive function or a function relative to the time that satisfies : $$a(t) > 0, \sum_{t=0}^{\infty} a(t) = \infty, \sum_{t=0}^{\infty} a(t)^2 < \infty$$
Step 1	At time t, apply the controller of eq. (13) during the time interval $[t, t + \delta t]$ and calculate $\varepsilon\left(x(t), \hat{P}\right)$ in eq. (15)
Step 2	Create a Linear In the Parameters (LIP) approximator of $\varepsilon\left(x(t), \hat{P}\right)$: $$\varepsilon\left(x(t), \hat{P}\right) = \theta^T \varphi\left(x(t); \hat{P}(t)\right)$$ $$\theta = argmin_\theta \sum_{i=t-\delta t T}^{t} \left(\varepsilon\left(x(i); \hat{P}(i)\right) - \theta^T \varphi\left(x(i); \hat{P}(i)\right)\right)^2$$ θ and φ are the vectors of parameter estimator and regression, respectively, while $T = min\left(\frac{t}{\delta t}, T_h\right)$
Step 3	Apply the controller of eq. (11) throughout the whole duration of the simulation and calculate $\hat{P}_{best}(t)$, which is the best matrix that has been found, until that point: $$\hat{P}_{best}(t) = \underset{P_j(s), s=0,\delta t, 2\delta t, \ldots, t}{\arg min} \left\{\sum_{t=0}^{T} \varepsilon_k \left(x(t); \hat{P}_k(s)\right)^2\right\}$$ So that $\hat{P}_{best}$ is the best matrix found so far that minimize the performance of the entire microgrid.
Step 4	Create *N* candidates (random perturbations) of the matrix $\hat{P}_{best}(t)$: $\hat{P}_{cand}{}^{(i)} = \left(1 - a(t)\right)\hat{P}_{best}(t) + a(t)\Delta\hat{P}^{(i)}$, i=1,2,…,N $\Delta\hat{P}^{(i)}$: random symmetric positive definite matrices P, that satisfy : $e_1 I \leq \Delta\hat{P}^{(i)} \leq e_2 I$
Step 5	The matrix that will be used by the controller (13) in the next time step is: $$\hat{P}(t + \delta t) = argmin_{\hat{P}_{cand}{}^{(i)}} \left\{\varepsilon\left(x(t), P_{cand}{}^{i}\right)\right\}^2$$
Step 6	Set t = t + δt and go to Step 1

3. The algorithm

It should be stressed here that, the previous equations are valid, a part from an approximation error *o(1/L)* due to the fact that the HJB equation is not solved exactly. When an approximation error is added in a gradient-based algorithm, it should be small enough so as not to destroy its convergence properties. The algorithm PCAO however "bypasses" the above problem, minimizing the effect of the approximation term. Therefore, PCAO can provide good solutions also in cases where the term *o(1/L)* is large. As mentioned earlier, to get to the optimal controller u^*, the optimal matrix P^* must be found. To do this, the algorithm first applies the control law

$$\hat{u} = \hat{u}\left(x(t); \hat{P}\right) \tag{13}$$

where $\hat{P}$ provides an estimation of the unknown matrix P^*. The next step is to find a way of measuring how far is this matrix from the optimal P^*. Integrating equation (12), the optimal performance of the system controller can be calculated, for a time $[t, t + \delta t]$, (where $\delta t > 0$, is a small discretization step):

$$\Delta V\left(x(t)\right) \approx -\int_t^{t+\delta t} \Pi\left(x(s)\right) ds + o\left({}^{1}/_{L}\right) \tag{14}$$

where $\Delta V\left(x(t)\right) = V\left(x(t+\delta t)\right) - V\left(x(t)\right)$. The error term, which results from the use of any other controller different from the optimum is defined as:

$$\varepsilon\left(x(t), \hat{P}\right) = \Delta \hat{V}(t) + \int_t^{t+\delta t} \Pi\left(x(s)\right) ds \tag{15}$$

Equation (15) can be interpreted as a way to know the distance of the matrix $\hat{P}$ from the optimum P^*. In order to minimize the term in (15) and consequently, the performance index, the matrix $\hat{\hat{P}}$ is updated at every iteration via the algorithm described in table II. The flow diagram of the PCAO algorithm is shown in figure 3. Figure 3 highlights the presence of a primary online feedback loop where the DG/DR decisions are tested in real-time, and of a secondary simulation-based feedback loop where the performance of candidate DG/DR strategies are assessed via the (EnergyPlus) simulation model of the microgrid. It can be shown that the PCAO algorithm converges asymptotically to the optimal matrix P^*. The interested reader is referred to [51,52] for the stability properties of the proposed algorithm.

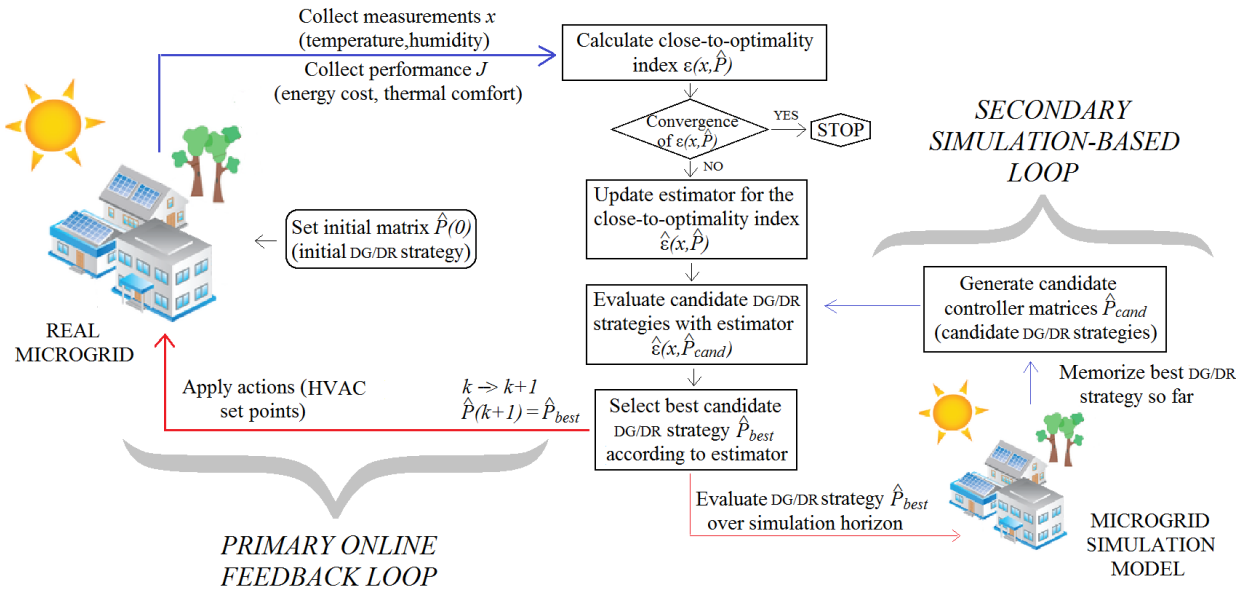

Figure 3. PCAO flow diagram

444

445 *4. Dimension of the microgrid problem*

446 In the microgrid under consideration the optimization algorithm must be able to handle the following state of
447 106 components:

448 • 3 external conditions: outdoor temperature, humidity and radiation;
449 • 12 predictions for the mean outside temperature and solar radiation for the next six hours;
450 • 60 measurements of temperature and humidity in each thermal zone of each building;
451 • 1 constant term (on the balance of the building);
452 • 30 operating set point temperatures of each HVAC in each thermal zone.

453 The total number of parameters that must be optimized corresponds to the elements of the symmetric matrix *P*
454 in the optimal quadratic Lyapunov function, which are

455 $$106 \times \frac{106+1}{2} = 5671$$

456 Thus the problem classifies as a large-scale one: besides it is nonlinear, due to the nonlinear microgrid
457 dynamics.

458 ## IV. Simulation Results

459 This section is devoted to analyse the performance of the proposed PCAO-based DG/DR control strategy as
460 compared with the four base case scenarios presented in section II.3. The four scenarios are useful to highlight
461 trade-offs between energy consumption and comfort (24^o C vs. 25^o C) and also to highlight the advantage of
462 sharing energy among buildings (isolated vs. connected setting). The performed simulations highlight the strong
463 interconnection between energy demand and generation, since the energy demand is dynamically changed in
464 such a way to exploit to the maximum extent the available solar energy. Energy consumption and thermal
465 comfort are strongly connected since the HVAC operation influence directly the energy absorbed, but also the
466 indoor climate. The figures and tables of this section will show the power consumption (in kW) and thermal
467 comfort (%) for each building and for the whole microgrid. The simulations have been run using historical data
468 from 3 days of July 2011 (July 5^{th} - 6^{th} - 7^{th}). The figures show the results only for one day (July 5^{th}), while the
469 tables collect the performance of the microgrid during the entire 3-day period. The results are organized
470 according to two groups: comparison of PCAO with the 24-isolated and the 25-isolated scenarios (with solar
471 energy delivered according to 55%-30%-15%), and comparison of PCAO with the 24-connected and 25-

connected scenarios (with solar energy distributed proportionally to the energy demand). The comparisons are made with respect to the controller obtained via the PCAO algorithm. Finally, in section IV.3 a more advanced DG/DR control strategy based on a genetic algorithm is used for comparisons.

1. Comparison with 24-isolated and 25-isolated

In this comparison the two base case scenarios distribute the solar energy according to the fixed proportion 30%-55%-15%, while PCAO distributes the solar energy proportionally to the energy demand of each building, according to the Kirchhoff's circuit laws. Table III shows the daily mean energy demand and the Fanger index during July 5^{th} - 6^{th} - 7^{th} for the aggregate microgrid under the different DG/DR control strategies. The total aggregate cost, which is the sum of the previous two terms, is also shown.

Table III. Simulation results (July 5^{th} - 6^{th} - 7^{th}). The values refer to the daily mean calculated over the three days for the aggregate microgrid. The red percentages indicate the cost increase with respect to the PCAO cost

Microgrid aggregate costs	**PCAO**	**24-isolated**	**25-isolated**	**Only DR (with isolated PV)**
Violation 10% power excess [min/day]	20 min	25 min	130 min	20 min
Violation 10% PPD threshold [min/day]	0 min	0 min	85 min	15 min
Energy [kWh]	15.8	20.7/**31.0%**	16.9/**7.0%**	18.8/**19.0%**
Discomfort [%]	4.3	4.5/**4.4%**	7.9/**83.7%**	5.8/**34.9%**
Total cost	20.1	25.2/**25.4%**	24.8/**23.4%**	24.6/**22.4%**

A comparison of the PCAO strategy with the two scenarios 24-isolated and 25-isolated reveals improvements (with respect to the total cost) ranging from 23.4% to 25.4%. Note that, because of the presence of loads that cannot be controlled, the improvements would be even bigger (ranging from 26% to 33% respectively) if only the power consumption due to controllable loads is considered. The last column of table III is also of interest: here the PCAO strategy is compared with a control strategy that optimizes the HVAC set points, but without exchanging any solar energy among the buildings: this is a control strategy that accomplishes only the demand response task, and it is thus called “Only DR”. Interestingly, despite the fact that this strategy outperforms the two scenarios 24-isolated and 25-isolated, it is far from optimal: the improvement of PCAO over this strategy is 22.4%. It is very interesting to note that the PCAO strategy achieves smaller power consumption and better thermal comfort at the same time: the reason for this performance will be explained in the section IV.2.

One of the reasons why PCAO can do better than “24-isolated” and “25-isolated” is related to the fact that sharing solar energy is beneficial to the aggregate microgrids. This can be understood from figure 4, which shows the 55%-30-15%, solar energy distribution against the energy distribution obtained by PCAO (before

6am and after 6pm the distribution is constant because the optimization is off). Because of the fact that the demand response of PCAO is highly dynamically changing through the day, the constant percentage of distributed generation cannot be optimal. The percentage of solar energy delivered to each building should also dynamically change, and this is one of the reasons why the results of the isolated base case scenarios are not optimal: figure 4 reveals that, with respect to PCAO, 24-isolated and 25-isolated deliver too much solar energy to buildings 1 and 3, and not enough solar energy to building 2. At the same time the optimal DG and DR tasks are highly connected: this is the reason why optimizing the HVAC set points without sharing energy (last column of table III) gives a far from optimal solution. Table III also reports to what extent some constraints are violated (in minutes/day): in particular, the constraints under consideration are the violation of 10% in instantaneous power excess and the violation of 10% in instantaneous PPD. Note that these constraints are tighter than the constraints (3) and (6): simulations reveal that (3), the violation of 15% in instantaneous power excess only occurs for 40 minutes in 25-isolated, and (6), the violation of 15% in instantaneous PPD never occurs. It is found that PCAO shapes the microgrid demand in such a way to have only for 10 minutes an excess of power of 10%: furthermore, the thermal comfort is always below the recommended threshold of 10%.

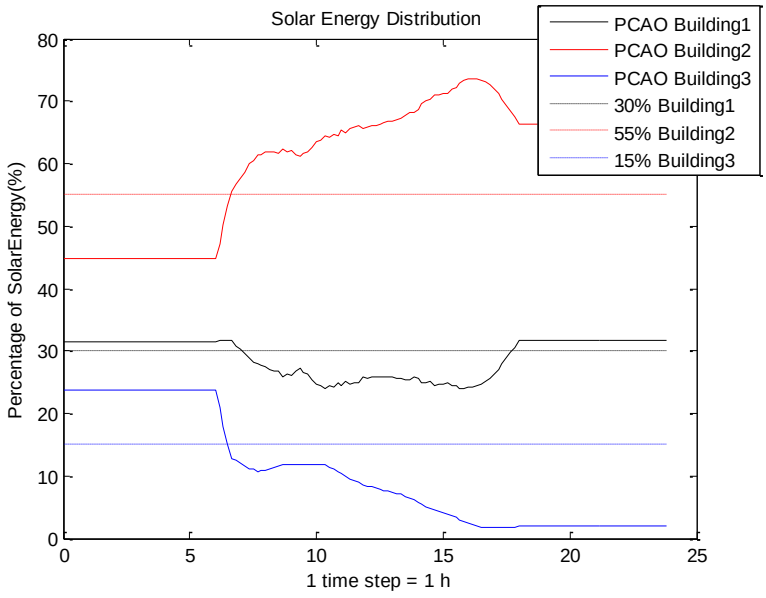

Figure 4. Solar energy distribution for each building under different control strategies: PCAO strategy (solid line) and isolated 30%-55%-15% strategy (dashed line). Before 6am and after 6pm the distribution of solar power is constant because no power consumption is occurring and the PCAO optimization is switched off.

2. Comparison with 24-connected and 25-connected

In this comparison each scenario distributes the solar power proportionally to the power demand of each building. Figures 4-5-6 show the behavior of the base scenarios as compared with the PCAO control strategy,

for each single building inside the microgrid. For better readability, the simulations refer only to July 5th. Even if the distribution of the solar energy according to the Kirchhoff's circuit laws lead to improved results over the proportional distribution 55%-30-15%, the PCAO strategy can still make a difference, due to the fact that it also dynamically shapes the energy demand of each building. Table IV reveals improvements ranging from 20.4% to 20.9%. The improvements would be even bigger (ranging from 25% to 30%, respectively) if only the power consumption due to controllable loads was considered. Table IV reveals that PCAO not only improves the total cost, but also the energy cost and the thermal cost singularly. This seems to violate the idea according to which improved thermal comfort requires more energy consumption: a close inspection of figures 5-6-7 reveals the intelligent mechanism that allows the PCAO strategy to improve both power and comfort cost.

Table IV. Simulation results (July 5th - 6th - 7th). The values refer to the daily mean calculated over the three days for the aggregate microgrid. The percentage indicates the cost increase (in red) or decrease (in blue) with respect to the PCAO cost

Microgrid aggregate costs	**PCAO**	**24-connected**	**25-connected**
Violation 10% power excess [min/day]	20 min	0 min	95 min
Violation 10% PPD threshold [min/day]	0 min	0 min	85 min
Energy [kWh]	15.8	19.8/**25.3%**	16.3/**3.2%**
Discomfort [%]	4.3	4.5/**4.4%**	7.9/**83.7%**
Total cost	20.1	24.3/**20.9%**	24.2/**20.4%**

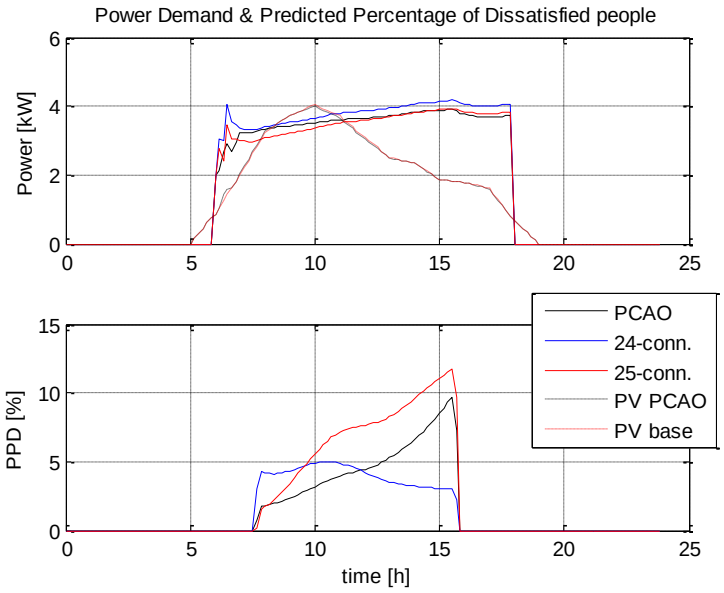

Figure 5. *Building 1*. Power demand and thermal comfort under different control strategies: PCAO (black solid line), 24-connected (blue solid line) and 25-connected (red solid line). The PV power is also shown (dashed lines).

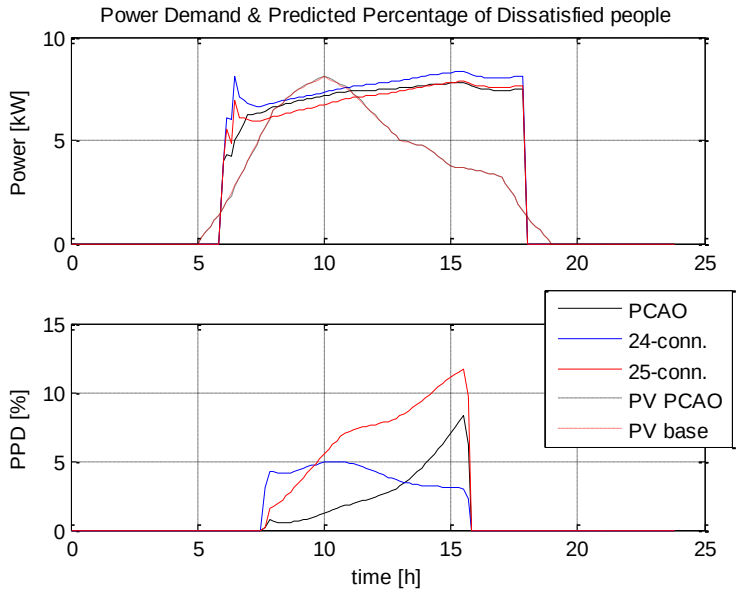

Figure 6. *Building 2*. Power demand and thermal comfort under different control strategies: PCAO (black solid line), 24-connected (blue solid line) and 25-connected (red solid line). The PV power is also shown (dashed lines).

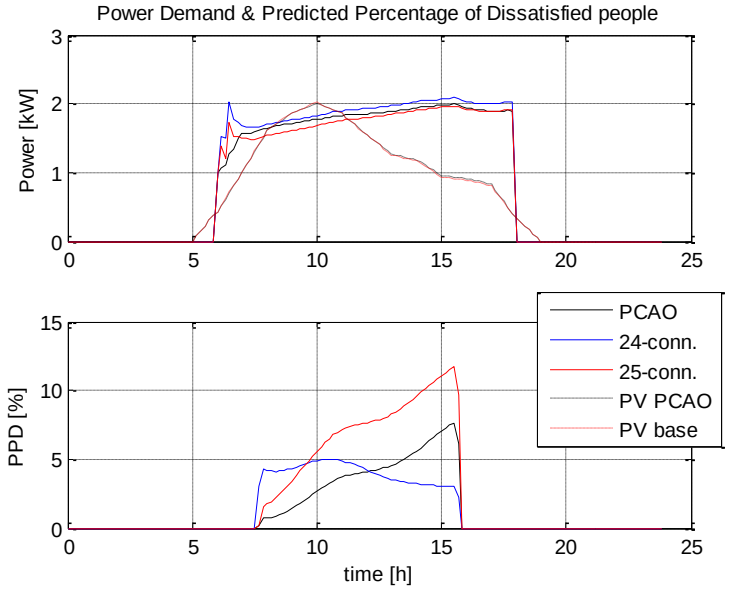

Figure 7. *Building 3*. Power demand and thermal comfort under different control strategies: PCAO (black solid line), 24-connected (blue solid line) and 25-connected (red solid line). The PV power is also shown (dashed lines).

Figures 5-6-7 show that the PCAO strategy shapes the power demand in the following way: late in the morning, when enough solar power is available, the HVAC units run at increased power so as to overcool the building and achieve a good PPD score. In the afternoon, when less solar power is available, PCAO sacrifices (in an optimal sense) the PPD index, because otherwise the buildings would be forced to absorb too much energy from the central grid. Notice that the power consumption of PCAO in the afternoon is smaller than the

power consumption of 24-connected and 25-connected.

Thus the PCAO strategy realizes that the buildings have a thermal inertia that can be exploited. This intelligent mechanism allows the minimization of the energy consumption (improvements ranging from 3.2% to 23.5%, respectively) and of the thermal discomfort (improvements ranging from 4.4% to 83.7%, respectively) at the same time. With the respect to the violation of constraints, it can be noted how, as expected, the isolated setting wastes more redundant power than the connected scenario.

3. Comparison with genetic algorithm

The proposed four base case scenarios are common practice DG/DR control strategies which employ simple rules: in order to compare the PCAO algorithm with a more advanced DG/DR control strategy, a genetic algorithm (implemented in the Matlab Optimization Toolbox [53] by the function ga) has been adopted to minimize the cost function (1). A genetic algorithm has been chosen, since this algorithm is adopted in many simulation-based approaches [54]. The genetic algorithm optimizes the cost function (1) in a simulation-based fashion, using a similar architecture as in figure 3. Three different implementation of the genetic algorithm have been tried: in the first one the genetic algorithm attempts to optimize the 5671 elements of the symmetric matrix P of the quadratic Lyapunov function. In the second implementation the genetic algorithm attempts to optimize the $106 \times 10 = 1060$ elements of the linear feedback vector K that maps the 106 variables of the feedback vector of section III.4 into the 10 control inputs. Unfortunately, both implementations led to unsatisfactory results. In fact, ever after thousands of iterations, the genetic algorithm was not able to provide relevant improvement with respect to the 24-connected and 25-connected strategies (improvements smaller than 2% have been found). This is probably due to the huge search space arising from the large number of parameters to be optimized. For this reason, a less computationally expensive open-loop DG/DR strategy has been implemented: by open-loop strategy it is meant that the DG/DR decide the daily profile of the HVAC set points not as a function of the state of the microgrid, but as the result of a receding-horizon optimization. In this third implementation of the genetic algorithm, the optimization is called to decide, from 6am to 6pm, the profile of 30 HVAC set points every 60 minutes: this profile results in $30 \times 12 = 360$ decision parameters, which can be better handled by the genetic algorithm. The results of the third implementation of the genetic algorithm are shown in table V. The PCAO algorithm can outperform the genetic algorithm by 10.1% in energy consumption, 18.6% in thermal comfort and 10.4% in total cost. Similar violations of power excess and PPD constraints are observed. The reasons for the sub-optimal performance of the genetic algorithm might be that 360 decision parameters is still a big search space for the genetic algorithm, and that the HVAC set points should be scheduled more often than every 60

minutes (due to its closed-loop feedback nature, the PCAO algorithm can act on the HVAC set points continuously).

Table V. Simulation results (July 5th - 6th - 7th). The values refer to the daily mean calculated over the three days for the aggregate microgrid. The red percentage indicates the cost increase with respect to the PCAO cost

Microgrid aggregate costs	PCAO	Genetic
Violation 10% power excess [min/day]	20 min	20 min
Violation 10% PPD threshold [min/day]	0 min	0 min
Energy [kWh]	15.8	17.4/**10.1%**
Discomfort [%]	4.3	5.1/**18.6%**
Total cost	20.1	22.5/**10.4%**

4. Computational time

The simulation section is concluded with considerations about the computational time of the proposed PCAO algorithm. A workstation with quad-core processor at 3.6 GHz, 10MB cache, RAM 8GB has been used for the simulations. Working with a linear-in-the-parameters estimator of dimension 15000, and with N = 5000 candidate DG/DR controllers, the time required at each iteration to train the estimator (step 2 of table II) is around 1 minute. The time needed for the simulation-based evaluation of the controller (step 3 of table II) requires running one EnergyPlus simulation: in 2-3 minutes it is possible to evaluate the performance of a controller over a horizon of 8-10 days. Finally, steps 4 and 5 of table II require another minute. The overall update iteration (i.e. the secondary loop of figure 3) is therefore feasibly implementable online adopting a time step of 10 minutes. It can also be considered that sometimes, because of safety reasons, the grid operator might prefer not to change DG/DR controller from one time step to the other, and might prefer keeping the same controller for the entire day. In such a situation, the PCAO strategy can be adopted as an offline optimization strategy. In this case both loops in figure 3 are performed offline and the optimization can run after 6pm outside occupancy hours, till convergence, using the data collected during the last day, and possible weather predictions based on historical data for the next day(s). In this offline mode it has been found that PCAO converges after around 4 to 5 hours of calculations, after which the optimal DG/DR strategy of the microgrid over the next 2 days is obtained. As compared with a genetic algorithm with a population of 5000 candidate controllers (the same number of candidate solution evaluated by the PCAO estimator), the computational time required to evaluate the performance index of the entire population is 2minutes/controller×5000controllers ≈ 7 days. In fact, the computational advantage of PCAO is that the candidate DG/DR strategies are evaluated by the

estimator, and only the best one is evaluated via an EnergyPlus simulation. The total computational time is thus drastically reduced. In order to reduce the computational effort of the genetic algorithm, the population of candidate DG/DR controllers has been reduced to 300 and, in order to obtain the results of table V, the genetic algorithm has been run for 1 week of calculations.

V. Conclusions

The paper presented a novel control algorithm for joint demand response and thermal comfort optimization in photovoltaic-equipped interconnected microgrids. The main contributions of the paper were: (a) contrary to many state-of the-art approaches that rely on simplified linear models, this paper employed a realistic nonlinear microgrid modelled, modelled in an elaborate energy building simulation program (EnergyPlus), for the synthesis and evaluation of the proposed control strategy; (b) the optimization was performed under a realistic thermal comfort model (Fanger index), and the thermal satisfaction of the end user is part of the performance index to be optimized; (c) the optimization of the energy demand via HVAC management is performed jointly with the solar energy distribution; it was also shown that HVAC management leads to far from optimal results if solar energy is not shared in the microgrid. Comparisons with rule-based DG/DR strategies have been performed; the proposed algorithm showed improvements ranging from 23.4% to 25.4% with respect to rule-based DG/DR strategies that do not share solar energy among buildings, and improvements ranging from 20.4% to 20.9% with respect to rule-based DG/DR strategies that share solar energy among buildings. While the base case scenarios achieved good thermal comfort only at the expense of very high energy consumption, or low energy consumption at the expense of unacceptable thermal comfort, the proposed optimization algorithm integrated the microgrid with the photovoltaic system and sensibly reduced dependence from the central grid. Improvements of 10.4% with respect to an alternative genetic-based DG/DR strategy have also been achieved. The proposed DG/DR strategy achieved the optimal between the following tasks; the energy absorbed from the main grid was reduced, the energy demand of each building was balanced with the solar energy, while taking into account the thermal comfort of the occupants. The intelligent mechanism leading to improved performance can be summarized as follows: while dynamically changing the HVAC set points, the proposed algorithm exploited the thermal inertia of the buildings to reduce the cooling action during the afternoon, when the solar energy decreases, because otherwise the buildings would be forced to absorb too much energy from the central grid. This intelligent mechanism was performed while improving at the same time the thermal comfort.

VI. Acknowledgements

The research leading to these results has been partially funded by the European Commission FP7-ICT-5-3.5, Engineering of Networked Monitoring and Control Systems, under the contract #257806 AGILE - http://www.agile-fp7.eu/ and FP7-ICT-2013.3.4, Advanced computing, Embedded Control Systems #611538 Local4Global - http://www.local4global-fp7.eu/.

VII. References

[1] H. Farhangi, "The path of the smart grid", *IEEE Power and Energy Magazine*, (8), (2010), pp. 18-28.
[2] N. Hatziargyriou, H. Asano, R. Iravani, and C. Marnay, C. , "Microgrids", *IEEE Power and Energy Magazine*, (5), (2007), pp. 78-94.
[3] O. Alsayegh, S. Alhajraf, and H. Albusairi, "Grid-connected renewable energy source systems: Challenges and proposed management schemes", *Energy Conversion and Management*, (51), (2010), pp. 1690-1693.
[4] A. Molderink, V. Bakker, M. Bosman, J. Hurink, and G. Smit, "Management and control of domestic smart grid technology". *IEEE Transactions on Smart Grid*, (1) (2010), pp. 109-119.
[5] G. Kyriakarakos, D. D. Piromalis, A. I. Dounis, K. G. Arvanitis, G., Papadakis. "Intelligent demand side energy management system for autonomous polygeneration microgrids". *Applied Energy* (103), (2013), 39–51.
[6] L. Zhang, N. Gari, and L. V. Hmurcik, "Energy management in a microgrid with distributed energy resources", *Energy Conversion and Management*, (78), (2014), pp. 297-305.
[7] X. Guan, Z. Xu, and Q.-S. Jia, "Energy-Efficient Buildings Facilitated by Microgrid" *IEEE Transactions on Smart Grid*, (1), (2010), pp. 243-252.
[8] D Zhang, N. Shah, and L. G. Papageorgiou, "Efficient energy consumption and operation management in a smart building with microgrid", *Energy Conversion and Management*, (74), (2013), pp. 209-222.
[9] A. Parisio, E. Rikos, G. Tzamalis, L. Glielmo. "Use of model predictive control for experimental microgrid optimization". Applied Energy (115), (2014), pp. 37–46.
[10] M. Marzband, A. Sumper, J. L. Dominguez-Garcia, R. Gumara-Ferret. "Experimental validation of a real time energy management system for microgrids in islanded mode using a local day-ahead electricity market and minlp". *Energy Conversion and Management* (76), (2013), pp. 314–322.
[11] D. Crawley, L. Lawrie, F. Winkelmann, W. Buhl, Y. Huang, C. Pedersen, R. Strand, R. Liesen, D. Fisher, and M. Witte, "EnergyPlus: creating a new-generation building energy simulation program", *Energy and Buildings*, (33), (2001), pp. 319-331.
[12] S. Klein, W. Beckman, and J. Duffie, "TRNSYS - A Transient Simulation Program", *ASHRAE Transaction,s* (82), (1976), pp. 623--633.
[13] D. Crawley, J. Hand, and M. Kummert, and B. Griffith, "Contrasting the capabilities of building energy performance simulation programs", *Building and Environment*, (43), (2008), pp. 661-673.
[14] M. Wetter, "Building Controls Virtual Test Bed". Lawrence Berkeley National Laboratory, (2011), available at http://simulationresearch.lbl.gov/bcvtb/releases/1.0.0/doc/manual/index.xhtml
[15] Z. Yu and A. Dexter. "Simulation based predictive control of low energy building systems using two-stage optimization" Proc. IBPSA09, (2009), pp. 1562–1568.
[16] M. Trcka, J. L. M. Hensen, and M. Wetter. "Co-simulation of innovative integrated HVAC systems in buildings", *Journal of Building Performance Simulation* (2), (2009), pp. 209–230.
[17] T. Nghiem and G. H. Pappas. "Receding-horizon supervisory control of green buildings", *American Control Conference*, San Francisco, CA, (2011).
[18] X. Xue, S. Wang, Y. Sun, F. Xiao. "An interactive building power demand management strategy for facilitating smart grid optimization". *Applied Energy* (116), (2014), pp. 297–310.
[19] R. Velik, P. Nicolay. "Grid-price-dependent energy management in microgrids using a modified simulated annealing triple-optimizer". *Applied Energy* (130), (2014), pp. 384–395.
[20] H. Zhang, E. Arens, C. Huizenga, T. Han. "Thermal sensation and comfort models for non-uniform and transient environments: Part I: Local sensation of individual body parts". *Building and Environment* (45), (2010), pp 380-388.
[21] H. Zhang, E. Arens, C. Huizenga, T. Han. "Thermal sensation and comfort models for non-uniform and transient environments: Part II: Local comfort of individual body parts". *Building and Environment* (45), (2010), pp 389-398.
[22] H. Zhang, E. Arens, C. Huizenga, T. Han. "Thermal sensation and comfort models for non-uniform and transient environments: Part III: Whole-body sensation and comfort". *Building and Environment* (45), (2010), pp 399-408.
[23] F. Oldewurtel, D. Sturzenegger, M. Morari. "Importance of occupancy information for building climate control". *Applied Energy* (101), (2013), pp. 521–532.
[24] European Committee for Standardization (CEN), "EN 15251 Indoor environmental input parameters for design and assessment of energy performance of buildings- addressing indoor air quality, thermal environment, lighting and acoustics". Brussels (2007).
[25] Communication from the Commission to the Council and the European Parliament, "Renewable Energy Road Map Renewable energies in the 21st century: building a more sustainable future, SEC(2006) 1719, SEC(2006) 1720, SEC(2007) 12.
[26] D. Kolokotsa, A. Pouliezos, G. Stavrakakis, and C. Lazos, "Predictive control techniques for energy and indoor environmental quality management in buildings", *Building and Environment*, (44), (2009), pp. 1850-1863.
[27] F. Oldewurtel, A. Parisio, C. N. Jones, D. Gyalistras, M. Gwerder, V. Stauch, B. Lehmann, and M. Morari, "Use of model predictive control and weather forecasts for energy efficient building climate control", *Energy and Buildings*, (45), (2012), pp. 15-27.
[28] J.D. Álvarez, J.L. Redondo, E. Camponogara, J. Normey-Rico, M. Berenguel, P.M. Ortigosa, "Optimizing building comfort temperature regulation via model predictive control", *Energy and Buildings*, (57), (2013), pp. 361-372.
[29] J. Wright, H. Loosemore, and R. Farmani, "Optimization of building thermal design and control by multi-criterion genetic algorithm", *Energy and Buildings*, (34), (2002), pp. 959-972.
[30] R. Z. Freire, G. H. C. Oliveira, and N. Mendes, "Predictive controllers for thermal comfort optimization and energy savings", *Energy and Buildings*, (40), (2008), pp. 1353–1365.

[31] ASHRAE, ANSI/ASHRAE Standard 55-2004: "Thermal environmental conditions for human occupancy", *American Society of Heating*, Refrigerating and air-Conditioning Engineers (2004).
[32] ENISO, 7730, "Moderate thermal environment: determination of the PMV and PPD indices and specification of the conditions for thermal comfort", International Organization for Standardization, Geneva, Switzerland, (2005).
[33] A. P. Gagge, A.P. Fobelets, and L.G. Berglund "A standard predictive index of human response to the thermal environment", *ASHRAE Transactions*, (92), (1986), pp. 709-731.
[34] N. Z. Azer and S. Hsu, "The prediction of thermal sensation from a simple model of human physiological regulatory response, *ASHRAE Transactions*, (83), (1977).
[35] L. Perez-Lombard, J. Ortiz, C. Pout. "A review on buildings energy consumption information". *Energy and buildings*, (40), (2008), pp. 394–398.
[36] S. Baldi, I. Michailidis, V. Ntampasi, E. B. Kosmatopoulos, I. Papamichail, and M. Papageorgiou, "Simulation-based Synthesis for Approximately Optimal Urban Traffic Light Management", *The 2015 American Control Conference*, July 1st–3rd, Chicago, IL, USA, 2015.
[37] A. Renzaglia, L. Doitsidis, A. Martinelli, and E. B. Kosmatopoulos. "Multi-robot 3d coverage of unknown areas", *International Journal of Robotics Research*, (31), (2012), pp. 738–752.
[38] D. Kolokotsa, D. Rovas, E. B. Kosmatopoulos, and K. Kalaitzakis. "A roadmap towards intelligent net zero- and positive-energy buildings", *Solar Energy*, (85), (2012), pp. 3067–3084.
[39] I. T. Michailidis, S. Baldi, E. B. Kosmatopoulos, M. F. Pichler, and J. R. Santiago "Improving Energy Savings and Thermal Comfort in Large-scale Buildings via Adaptive Optimization" in *Control Theory: Perspectives, Applications and Developments*, F. Miranda (editor), Nova Science Publishers, 2015.
[40] I. Michailidis, S. Baldi, E. B. Kosmatopoulos, and Y. S. Boutalis, "Optimization-based Active Techniques for Energy Efficient Building Control Part II: Real-life Experimental Results", *International Conference on Buildings Energy Efficiency and Renewable Energy Sources*, BEE RES 2014, June 1st-3rd, Kozani, Greece, 2014, pp. 39--42.
[41] J. A. Jardini, C. M. V. Tahan, M. R. Gouvea, S. Un Ahn, and F. M. Figueiredo, "Daily Load Profiles for Residential, Commercial and Industrial Low Voltage Consumers", IEEE Transactions on Power Delivery (15), (2000), pp. 375-380.
[42] Department of Energy, U. S., 2008. Energyplus energy simulation software. http://apps1.eere.energy.gov/buildings/energyplus/.
[43] K. Tanaka, A. Yoza, K. Ogimi, A. Yona, T. Senjyu. "Optimal operation of DC smart house system by controllable loads based on smart grid topology", Renewable Energy (39), (2012), pp. 132-139.
[44] I. Hadjipaschalis, A. Poullikkas, V. Efthimiou. "Overview of current and future energy storage technologies for electric power applications". *Renewable and Sustainable Energy Reviews* (13), (2009), pp. 1513–1522.
[45] D. Lindley. "Smart grids: The energy storage problem". *Nature* (463), (2010), pp. 18–20.
[46] R.E Bellman: *Dynamic Programming, Princeton* (1957).
[47] E. B. Kosmatopoulos and A. Kouvelas. "Large-scale nonlinear control system fine-tuning through learning", *IEEE Transactions Neural Networks*, (20), (2009), pp. 1009–1023.
[48] C. D. Korkas, S. Baldi, I. Michailidis, E. B. Kosmatopoulos. "Intelligent energy and thermal comfort management in grid-connected microgrids with heterogeneous occupancy schedule" *Applied Energy*, (2015), in press.
[49] S. Baldi, I. Michailidis, E. B. Kosmatopoulos, A. Papachristodoulou, P. A. Ioannou. "Convex Design Control for Practical Nonlinear Systems, IEEE Trans. on Automatic Control, (59), (2014), pp. 1692-1705.
[50] E. B. Kosmatopoulos, "An adaptive optimization scheme with satisfactory transient performance", *Automatica*, (45), (2009), pp. 716-723.
[51] S. Baldi, I. Michailidis, E. B. Kosmatopoulos, and P. A. Ioannou, "A "Plug-n-Play" Computationally Efficient Approach for Control Design of Large-Scale Nonlinear Systems using co-Simulation", *52nd IEEE Conference on Decision and Control, Florence, Italy, (2013)*.
[52] S. Baldi, I. Michailidis, E. B. Kosmatopoulos, and P. A. Ioannou, "A "Plug-n-Play" Computationally Efficient Approach for Control Design of Large-Scale Nonlinear Systems using co-Simulation", *IEEE Control Systems Magazine*, (34), (2014), pp. 56-71.
[53] T. F. Coleman, Y. Zhang, *Optimization Toolbox User's Guide*, Version 6.3, The MathWorks, Inc., Natick, MA, 2013.
[54] P. H. Shaikh, N. Bin Mohd Nor, P. Nallagownden, I. Elamvazuthi, and T. Ibrahim, "A review on optimized control systems for building energy and comfort management of smart sustainable buildings", *Renewable and Sustainable Energy Reviews* (34), (2014), pp. 409-429.